

PACS numbers: 47.57.jd, 61.48.De, 68.37.Og, 68.43.-h, 68.65.-k, 81.05.ub, 82.65.+r

Comparative Study of Ni(II) and Cu(II) Adsorption by As-Prepared and Oxidized Multi-Walled N-Doped Carbon Nanotubes

Renata Balog¹, Viktoria Simon², Maryna Manilo³, Laszlo Vanyorek³, Zoltan Csoma¹, and Sandor Barany^{1,3,4}

¹*Ferenc Rakoczi II. Transcarpathian Hungarian Institute,
6 Kossuth Square,
UA-90200 Beregszász, Transcarpathia, Ukraine*

²*F. D. Ovcharenko Institute of Biocolloidal Chemistry, N.A.S. of Ukraine,
42 Academician Vernadsky Blvd.,
UA-03142 Kyiv, Ukraine*

³*Institute of Chemistry, University of Miskolc,
Miskolc-Egyetemvaros,
3515 Miskolc, Hungary*

⁴*MTA-ME Materials Science Research Group,
Miskolc-Egyetemvaros,
3515 Miskolc, Hungary*

The laws and mechanisms of adsorption of Ni(II) and Cu(II) ions by well-characterized as-prepared and oxidized N-doped multi-walled carbon nanotubes (N-CNTs) are described and discussed. The samples are synthesized by catalytic chemical vapour deposition method using *n*-butylamine as carbon source and Ni(NO₃)₂ + MgO as catalyst and purified by treatment with HCl. The surface functionalization is performed using oxidation with mixture of concentrated H₂SO₄ and HNO₃. As shown, adsorption of Ni(II) and Cu(II) reaches equilibrium value within 20–30 min; adsorption results in a moderate decrease in the suspension pH for pristine N-CNTs (1.0–1.5 pH unit) and a considerable lowering the pH for oxidized sample (up to 2.5 pH unit); the adsorption isotherms are described by the Langmuir equation; the plateau amounts of adsorption (25–30 mg/g for Cu and 35–40 mg/g for Ni) are almost the same for both as-prepared and oxidized samples; at pH 8.0 and higher for Ni and pH 6.5 and higher for Cu ions, a sharp increase in adsorption is observed that is caused by the hydroxides' precipitation. The spectroscopic, adsorption, electrophoretic and pH measurements' data testify that below pH of hydroxide precipitation, the major mechanism of adsorption by as-prepared N-CNTs is the donor–acceptor interaction between the free electron pair of N atoms incorporated into nanotubes' lattice and vacant *d*-orbital of the adsorbing Ni(II)

or Cu(II) ions. For the oxidized N-CNTs, ion-exchange processes with a release of H^+ may play minor role.

В роботі розглянуто закони та механізми адсорбції йонів Ni(II) та Cu(II) охарактеризованими вихідними та окисненими N-легованими багатостінними вуглецевими нанорурками (N-CNT). Зразки синтезували методом каталітичного хемічного осадження пари *n*-бутиламіну як джерела Карбону та $Ni(NO_3)_2 + MgO$ як каталізатора з подальшою очисткою їх HCl. Функціоналізацію поверхні N-CNT проводили за допомогою окиснення сумішшю концентрованих H_2SO_4 та HNO_3 . Було показано, що: адсорбція йонів Ni(II) та Cu(II) досягає рівноважного значення протягом 20–30 хв.; адсорбція приводить до помірного зменшення рН суспензії для вихідних (1,0–1,5 одиниці рН) та значного пониження рН (до 2,5 одиниць рН) для окиснених N-CNT-зразків; ізотерми адсорбції описуються Ленгмюровим рівнянням; положення плато адсорбції (25–30 мг/г для Cu та 35–40 мг/г для Ni) майже однакове як для вихідних, так і для окиснених зразків; при $pH \geq 8,0$ для йонів Ni та $pH \geq 6,5$ для йонів Cu спостерігається різке збільшення величини адсорбції за рахунок осадження гідроксидів. Дані спектроскопічних, адсорбційних, електрофоретичних і рН-мірянь свідчать про те, при рН, нижчих за значення, при якому відбувається осадження гідроксидів, основним механізмом адсорбції вихідними N-CNT є донорно-акцепторна взаємодія між вільною парою електронів атомів Нітрогену, розміщених на ґратниці нанорурок, та вакантною *d*-орбіталлю йонів Ni(II) або Cu(II) відповідно. Для окиснених N-CNT процеси йонообміну з вивільненням H^+ відіграють незначну роль.

В работе рассмотрены законы и механизмы адсорбции ионов Ni(II) и Cu(II) охарактеризованными исходными и окисленными легированными азотом многослойными углеродными нанотрубками (N-CNT). Образцы синтезировали методом каталитического химического осаждения паров N-бутиламина (источник углерода) и $Ni(NO_3)_2 + MgO$ (катализатор) с последующей их очисткой HCl. Функционализация поверхности N-CNT проводилась с помощью окисления смесью концентрированных H_2SO_4 и HNO_3 . Было показано, что: адсорбция ионов Ni(II) и Cu(II) достигает равновесного значения в течение 20–30 мин; адсорбция приводит к умеренному уменьшению рН суспензии на исходных (1,0–1,5 единицы рН) и значительному снижению рН (до 2,5 единиц рН) для окисленных N-CNT-образцов; изотермы адсорбции описываются уравнением Ленгмюра; положение плато адсорбции (25–30 мг/г для Cu и 35–40 мг/г для Ni) почти одинаково как для исходных, так и для окисленных образцов; при $pH \geq 8,0$ для ионов Ni и $pH \geq 6,5$ для ионов Cu наблюдается резкое увеличение величины адсорбции за счёт осаднения гидроксидов. Данные спектроскопических, адсорбционных, электрофоретических и рН-измерений показывают, что при рН ниже значения, при котором происходит осаднение гидроксидов, основным механизмом адсорбции исходными N-CNT является донорно-акцепторное взаимодействие между свободной парой электронов атомов азота, размещённых на решётке нанотрубок, и вакантной *d*-орбиталью

ионов Ni(II) или Cu(II) соответственно. Для окислённых N-CNT процессы ионообмена с высвобождением H^+ играют незначительную роль.

Key words: N-doped multi-walled carbon nanotubes, Ni(II) and Cu(II) ions, adsorption, kinetics.

Ключові слова: N-леговані багатопарові вуглецеві нанорурки, йони Ni(II) та Cu(II), адсорбція, кінетика.

Ключевые слова: N-легированные многослойные углеродные нанотрубки, ионы Ni(II) и Cu(II), адсорбция, кинетика.

(Received 4 December, 2019; in final version, 31 January, 2020)

1. INTRODUCTION

Among variety of practical applications of carbon nanotubes (CNTs), an increasing important segment is related to their use as sorbents for toxic substances, heavy metal ions, and organic compounds [1]. For example, CNTs are intensely studied as sorbents for water purification from individual nickel and lead [2], copper and cobalt [3], chromium [4] ions, and other individual or mixed ions of different metals [5].

Nickel (II) is a hazardous heavy metal ion, which is increasingly accumulated in potable, ground and wastewaters. Copper is an essential nutrient, for which the World Health Organization (WHO, 1998) recommends a daily intake of 30 $\mu\text{g}/\text{kg}$ body weight. Drinking water standards have been established to prevent adverse health effects resulting from ingestion of too much copper. WHO (1998) recommends a limit of 2 mg/dm^3 Cu to prevent adverse health effects from copper exposure. There are numerous studies devoted to extraction of these ions by single-walled (SWCNTs) or multi-walled carbon nanotubes (MWCNTs), both pristine and oxidized by different agents. The kinetics of adsorption, shape of adsorption isotherms, impact of pH and degree of CNT surface functionalization has been elucidated. A short review of the recent results obtained is summarized below.

Authors [6, 7] have shown that the adsorption of Ni(II) onto oxidized CNTs is strongly dependent on pH and nanotubes concentration and, to a lesser extent, ionic strength. The adsorption data well fit the Langmuir model, and the adsorbed Ni(II) can be easily desorbed at $\text{pH} < 2.0$. It was speculated that ion exchange might be the predominant mechanism of Ni(II) adsorption on oxidized CNTs. Adsorption of Ni(II) on oxidized CNTs was increased from zero to 99% at $\text{pH} 2.0\text{--}9.0$ and then maintained the high level with increasing pH. The adsorption achieved equilibrium within 2 h [7].

The mechanism of adsorption was attributed to surface complexation and ion exchange. It was also shown that the adsorption capacity for nickel ions from aqueous solutions increased significantly onto the surface of the oxidized CNTs compared to that on the as-produced CNTs, and the maximum adsorption by these adsorbents was determined as 18.08 and 49.26 mg/g, respectively [8]. The number of functional groups, total acidic sites and negatively charged carbons on CNTs surface were greatly increased after oxidation by NaOCl, which resulted in sorption of more Ni ions [9]. Typically, 60–95% of Ni(II) can be extracted from aqueous solution by MWCNTs depending on the initial solution concentrations [10]. As suggested by the distribution coefficient values, increased initial Ni(II) solution concentrations resulted in lower adsorption, while the total amount of ions removed from the equilibrating solutions increased.

Higher adsorption was observed at $\text{pH} > 6.0$, and the sorption process reached equilibrium at 60 min. The sorption mechanisms are complicated and appear attributable to electrostatic forces and chemical interactions between the nickel ions and the surface functional groups of the CNTs [10].

Carbon nanotubes were shown to possess good adsorption properties and high capacity (3.5 mg/g at initial concentration of Cu^{2+} ions of 20 mg/dm^3) in respect to Cu(II) ions. The affinity of this ion to the CNT surface and the adsorbed amounts were found to be higher compared to other heavy metal ions such as Co, Zn, Pb, Mn. The adsorption data were well described by the Freundlich isotherm [11].

The adsorption capacity of oxidized N-doped bamboo like MWCNTs in respect to Cu(II) ions reached 15 mg/g [12]. Authors [13, 14] have shown that the interaction of Cu(II) ions deposited on the N-CNT surface by thermal decomposition of copper acetate is realized via their strong coordination by pyridine nitrogen atoms at the edge of the graphene sheets of the adsorbent reviewed the laws and mechanisms of sorption of divalent metal ions (Cd^{2+} , Cu^{2+} , Ni^{2+} , Pb^{2+} , and Zn^{2+}) from aqueous solution by various kinds of raw and surface oxidized carbon nanotubes. The sorption mechanisms appear mainly attributable to chemical interactions between the metal ions and the surface functional groups of the CNTs. The sorption capacities of CNTs remarkably increased after oxidized by NaOCl, HNO_3 and KMnO_4 solutions and reached, for example, 6.9 Ni mg/g and 47.8 Ni mg/g onto CNTs oxidized by HNO_3 or NaOCl, respectively. Similar results were obtained by authors [15], who have shown that MWCNTs can be successfully used for the removal of heavy metals from aqueous solution. A competition among the metal ions for binding was revealed on the MWCNTs surface with affinity in the

order: Cu(II) > Zn(II) > Pb(II) > Cd (II). Authors [16] have analysed in detail the impact of CNTs properties (adsorption sites, pore volume, BET surface area, surface total acidity) and solution properties (ionic strength, effect of pH) on the adsorption of heavy metal ions by carbon nanotubes. The contribution of physical adsorption, electrostatic attraction, precipitation and chemical interaction between the metal ions and the surface functional groups of CNTs was discussed.

Gao *et al.* [17] measured the adsorption isotherms of Cu(II), Ni(II), Zn(II) and Cd(II) onto carbon nanotubes oxidized by concentrated HNO₃ in single, binary, ternary and quaternary systems, and have shown that isotherms reveal the effect of competition for adsorption sites seen as a decrease in the amount adsorbed. The uptakes at the equilibrium concentration of 0–0.04 mmole/dm³ in single system and 0–0.15 mmole/dm³ in binary system are in the order Cu²⁺ > Ni²⁺ > Cd²⁺ > Zn²⁺ while for the ternary and quaternary, the order is Cu²⁺ > Cd²⁺ > Zn²⁺ > Ni²⁺.

Summarizing the literature review, we can say that the major factors affecting the adsorption of Ni(II) and Cu(II) by carbon nanotubes and the mechanisms of the process are at large clarified. At the same time, surprisingly, there is a lack of information about the laws and mechanisms of adsorption of these ions by N-doped carbon nanotubes, *i.e.* adsorbents containing surface N atoms in different state, potentially capable to form complexes with Ni(II) and Cu(II) ions. We tried to fill in, at least in part, this gap.

2. MATERIALS AND METHODS

2.1. Materials

2.1.1. Synthesis and Functionalization of N-Doped Carbon Nanotubes

The N-doped carbon nanotubes (N-CNTs) were synthesized by catalytic Chemical Vapour Deposition method using n-butylamine (VWR) as carbon source and Ni(NO₃)₂·6H₂O (Sigma Aldrich) plus magnesium oxide, MgO (Merck) as catalyst materials, as described in the paper [12]. The product was purified from the catalyst by treatment with concentrated hydrochloride acid (VWR). The surface functionalization of N-CNTs was performed using oxidation with mixture of concentrated sulphuric acid and nitric acid (*V/V* = 3:1) at 80°C overnight using continuous stirring. After the acidic treatment, the N-CNTs were filtered and washed with distilled water until pH 5.0–6.0 was reached, then dried at 120°C. The mixture of H₂SO₄ and HNO₃ turned out to be very efficient for oxidation of carbon nanotubes, as it was shown in our previous work [18].

2.1.2. Characterization of N-Doped Carbon Nanotubes

The image of the N-CNTs obtained by High Resolution Transmission Electron microscopy—HRTEM (FeiTechnai G2, 200 kV) was shown in Fig. 1. Figure 1, *a* shows that non-oxidized N-CNTs represent uneven fibres with length of 2–3 μm , and diameter between 7 nm and 22 nm, with a mean value of 12.4 nm. As a result of oxidative treatment, the N-CNTs fibres were broken into shorter fibres, with about 200–800 nm sections in length (Fig. 1, *b*). This can be attributed to the fact that the N-doped bamboo-like carbon nanotubes are easily ruptured, because their mechanical strength is lower compared to their non-doped counterparts.

The extraordinary structure of these nanotubes is demonstrated on their schematic illustration (Fig. 1, *c*). A number of graphene edges are seen on the wall of N-CNTs, containing sp^3 carbon atoms and nitrogen atoms, which easily react with oxidants (Fig. 1, *d*). In this sense, the N-CNTs can be oxidized to higher extent than the non-doped, conventional MWCNTs or SWCNTs. The fibre edges can serve as high energy adsorption sites on the wall of bamboo-like nanotubes, which are easily accessible for different ions or molecules and can form relatively strong bounds with the adsorbent surface (due to ion exchange adsorption, surface complexes or π - π interactions).

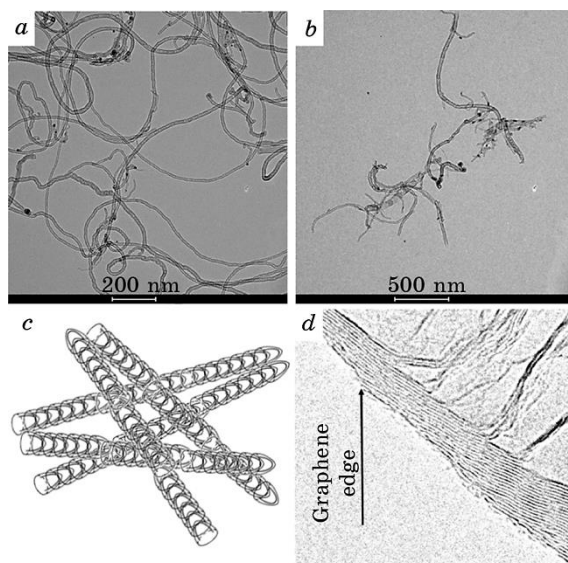


Fig. 1. HRTEM image of the non-oxidized (*a*) and oxidized (*b*) N-CNTs; schematic illustration of the bamboo-like structure (*c*); the graphene edges on the CNTs wall (*d*).

X-Ray Photoelectron Spectroscopy—XPS (SPECS instrument with PHOIBOS 150 MCD 19 detector) and Fourier-transform infrared spectroscopy—FTIR (A VERTEX 70 FTIR spectrometer, Bruker, Germany) measurements were applied to identify the binding types and the nature of surface functional groups.

Figure 2 shows the XPS spectra of the non-oxidized and oxidized N-CNTs characterizing the binding energy of the C–N and C–O bounds. The peak at 398.6 eV binding energy can be attributed to the pyridine type nitrogen atoms (Fig. 2, *a*), the next peak at 401.1 eV originates from the graphitic nitrogen incorporation. A peak of the oxidized nitrogen (pyridine N⁺–O[–] species) can be also observed on the spectrum at the binding energy of 404.7 eV. The N-doped CNTs are easily oxidized at crystal distortions in the graphitic structure. During the acidic treatment oxygen containing functional groups are developed, which are located at the C1s band (Fig. 2, *b*). The appearance of –C=C– and –C–C– bounds is reflected by a highly intensive peak at 284.6 eV, and the C=O peak was identified at

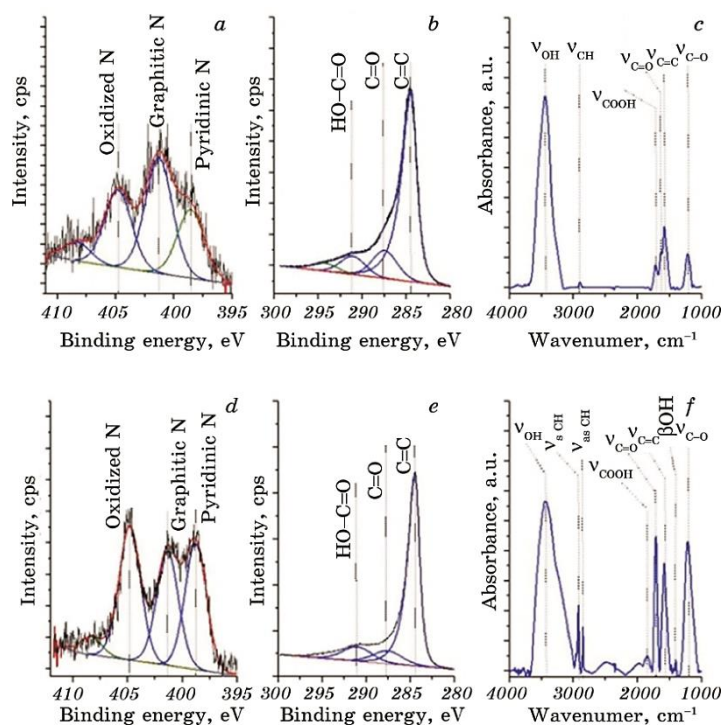


Fig. 2. XPS spectra with deconvoluted N1s band of the non-oxidized (*a*) and oxidized (*d*) N-CNTs and C1s band of the non-oxidized (*b*) and oxidized (*e*) N-CNTs. FTIR spectrum of the non-oxidized (*c*) and oxidized (*f*) N-CNTs.

287.5 eV (Fig. 2, *b*). The peak of the carboxyl groups is shown at the binding energy of 291.2 eV. These oxygen-containing functional groups are visible on the FTIR spectra (Figs. 2, *c*, *f*): stretching vibration of the C–O bond at 1205 cm^{-1} , carbonyl bond at 1628.7 cm^{-1} , carboxyl groups at 1713.7 cm^{-1} and hydroxyl groups at 3440.7 cm^{-1} (Fig. 2, *c*). The latter bond is originated from the alcoholic or phenolic hydroxyl groups and from the –COOH groups. Adsorbed water can contribute to the appearance of this absorption bond as well. The vibration mode of N-CNT structure ($\nu_{\text{C=C}}$) was also found in the FTIR spectrum at 1565.4 cm^{-1} wave number.

ZetaSizer Nano ZS instrument (Malvern, United Kingdom) was used for determination of the electrophoretic mobility of N-CNTs in aqueous media (0.01% wt., here-and-after %) at room temperature ($T = 298\text{ K}$) in the range of external electric field gradients of 6–15 V/cm. The electrophoretic mobility was transformed into ζ -potential using the classical Smoluchowski equation approach with the software of the instrument. The presented values of the ζ -potential were obtained by averaging three to six measurement results; the measurements error was about 3–5%.

Figure 3 shows the pH-dependence of N-CNTs electrokinetic potential in aqueous suspension. For the pristine N-CNT samples, the isoelectric point (IEP) is observed near pH 7.2, which is higher than the IEP values reported for regular (no N atoms in the lattice) N-CNTs: pH 4.0 [19] or pH 6.0 [20]. This means that at lower pH, the surface is charged positively. The positive charge of the surface in acidic media (pH 3–7) is due to the presence of small amounts of

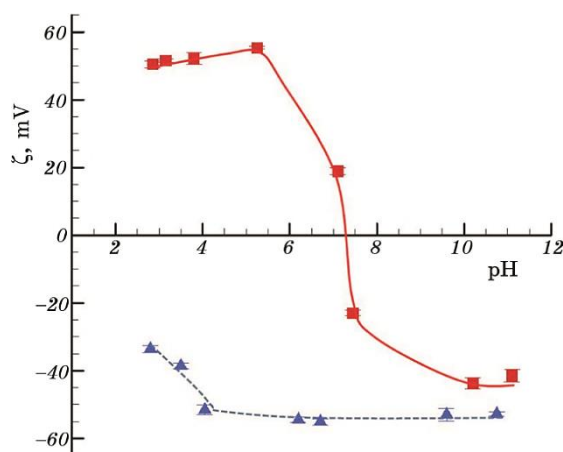


Fig. 3. Dependence of the ζ -potential of the pristine (squares) and oxidized (triangles) N-CNTs on the system pH. Concentration of N-CNTs was 0.01%.

oxidized species in the original N-CNTs (see spectra in Fig. 2) as well as to the presence of pyridine type N atoms in the lattice capable to acquire positive charge due to proton transfer. The shift of the IEP to higher values probably reflects the contribution of protonated N-atoms into the CNTs surface charge. After the acid treatment, the IEP is not reached, and the surface charge remains negative in the whole pH interval studied (pH 3–12). This is due to the dissociation of oxidized negative species of various natures on the N-CNTs surface. An increase in the number of oxidized specimens and a decrease in the number of low-oxidized groups formed on the surface overcompensate the contribution of the positive surface charge.

2.2. Methods: Adsorption Measurements

Ni(II) and Cu(II) ions were adsorbed by the carbon nanotubes (typical adsorbent concentration of 0.1%) at room temperature in a pH range of 2.0–12.0 under mechanical shaking the reaction mixtures for designated period of time. The kinetic dependencies were measured during 36 h. The concentration of nickel and copper ions before and after adsorption was determined in acetylene–air flame with an Agilent 240AA atomic absorption spectrophotometer (Agilent Technologies, US) operating at a wavelength of 429.0 nm and an optical gap width of 0.5 nm. The chosen conditions enable to determine the concentration of Ni(II) ions in the range of 1–100 $\mu\text{g}/\text{dm}^3$. The adsorbed amount was calculated from the material balance of ions in solution prior and after adsorption.

3. RESULTS AND DISCUSSION

3.1. Kinetics of Adsorption

Figure 4 demonstrates the time dependencies of adsorption of Ni(II) and Cu(II) ions by pristine and oxidized N-CNTs at pH 5.5. The kinetics of adsorption of heavy-metal ions by carbon-containing sorbents is a rather complex process. Most works consider a two-step adsorption kinetics, *i.e.*, an initial rapid uptake and a much slower second stage of adsorption, which may last for several days and even weeks [21–24]. Some authors reported an optimal contact duration of several minutes [24], while others believe that the optimal time required to establish equilibrium is several hundred hours [21, 23]. Generally, most authors suppose the optimal contact time to be 1–5 h [21, 22].

Three regions can be distinguished on the kinetic dependences of

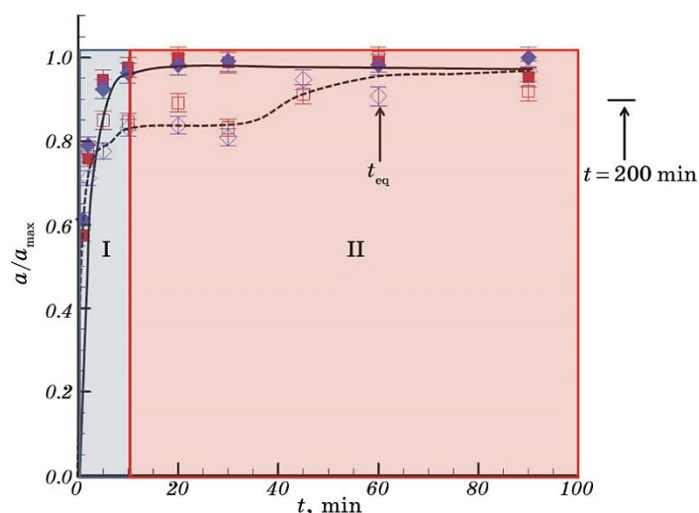


Fig. 4. Time dependences of Ni(II) (filled symbol) and Cu(II) (empty symbol) adsorption by the as-prepared (squares) and oxidized (diamonds) N-doped CNTs at pH 5.5.

adsorption of Ni(II) and Cu(II) in our experiments. At N-CNTs–solution contact duration $t \leq 10$ min (region I), the specific adsorption drastically increases with time; in a contact-time range of 10–100 min (region II), the adsorption equilibrium is established; at $t > 100$ min, Ni(II) ions are in a small amount (up to 10%) desorbed from the nanotubes surface and saturation in the adsorption was observed (region III). A further increase in the contact time up to 5 days gave an insufficient change (2–3%) in the adsorbed amount. Similar results were obtained while adsorbing Cr (III) ions on the CNTs surface [25]. Contact time $t_{\text{eq}} = 60$ min was chosen to measure the equilibrium adsorption isotherms. The data in Fig. 5 show that this time is enough to establish adsorption equilibrium.

3.2. Effect of pH

To estimate the role of ion-exchange processes in the mechanism of adsorption of Ni(II) and Cu(II) ions by N-CNTs, it is useful to inspect the changes in the suspension pH as a result of adsorption of ions. Inspecting the effect of pH on the adsorption of Ni(II) and Cu(II) ions by carbon nanotubes, quite different effects should be considered as follow.

(i) Ni(II) and Cu(II) ions in aqueous solutions are hydrated by six water molecules, they possess moderate resistance to hydrolysis. Nickel ions predominantly exist in the form of species with charge

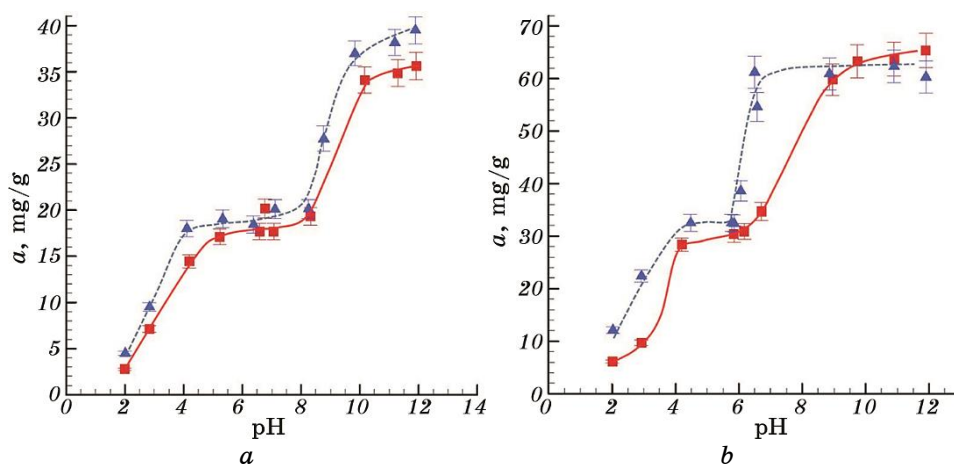


Fig. 5. pH-dependence of the nickel (a) and copper (b) ions' adsorption by as-prepared (squares) and oxidized (triangles) N-CNTs.

$2+$ in dilute solutions and hydrolysis products of $\text{Ni}(\text{OH})^+$ (the equilibrium constant of formation was determined as -19.8 [26] were found at concentration of salts higher than $5 \cdot 10^{-2}$ M of Ni(II) [27]. The type of specimen of copper ions also depended of their concentration and pH value of solution, *i.e.*, at low concentrations, the dominant species is the copper ion, Cu^{2+} (up to pH 7.5), copper hydroxide, $\text{Cu}(\text{OH})_2$ (up to pH 12.3) and $\text{Cu}(\text{OH})_3^-$ (pH 12.3). At higher copper concentrations, solid $\text{Cu}(\text{OH})_2$ is formed and precipitates out of solution at copper concentrations above the solubility product of copper hydroxide at $1 \cdot 10^{-8}$ M. It is important to note that the domain of stability of solid $\text{Cu}(\text{OH})_2$ is expanding to lower and higher pH values with increasing copper concentration. A small but significant amount of an important Cu(II) complex $\text{Cu}(\text{OH})^+$ is formed at low pH (3–7) [25]. Obviously, hydrolysis of nickel and copper salt with a release of H^+ ions results in a change of the surface charge of N-CNTs (see above) and possibly the adsorption of Ni(II) or Cu(II) ions.

(ii) Increasing the system pH gives a rise to the negative surface charge density of N-CNTs and to the adsorption of the positively charged nickel or copper ions *via* electrostatic mechanism.

(iii) at pH 6.5 or pH 7.8–8.0, the process of precipitation of $\text{Cu}(\text{OH})_2$ or $\text{Ni}(\text{OH})_2$, respectively, starts [26] that leads to pseudo-adsorption of the metal ion on the nanotubes surface.

The dependences of Ni(II) and Cu(II) adsorption on the adjusted pH values by N-CNTs are shown in Fig. 5. In acidic media (from pH 2.0 to pH 4.0), a marked rise in adsorption with an increase in pH was observed; then in the interval of pH 4.0–8.0 for Ni(II) or pH

4.0–6.5 for Cu(II), a roughly constant value of adsorption was measured. After that, a sharp elevation in the Ni(II) and Cu(II) adsorption took place due to precipitation of nickel and copper hydroxide on the surface. The adsorbed amount of both ions by oxidized samples is higher compared to that by as-prepared nanotubes in the almost whole pH interval studied. This is explained by additional contribution of the ion exchange to the mechanism of adsorption in the first system (see below).

Figure 6 demonstrates the adsorption isotherms of the Ni(II) and Cu(II) ions onto as-prepared and oxidized N-CNTs measured at ‘natural’, *i.e.*, non-adjusted pH. In addition, the changes in the equilibrium pH of suspensions because of adsorption of heavy metal ions are depicted in Fig. 6. It is seen that the shape of adsorption isotherms is similar: a stepwise rise in adsorption with increasing the equilibrium concentration of the nickel or copper ions, with a tendency to reach a plateau value of the adsorbed amount (Langmuir type isotherm); the maximum adsorbed amount slightly increases while moving from as-prepared (28 mg/g for Cu and 35 mg/g for Ni) to oxidized (36 mg/g for Cu and 40 mg/g for Ni) samples; adsorption of these ions gives a moderate lowering in the solution pH for pristine N-CNTs (up to 1.0–1.5 pH unit) and a marked drop for oxidized sample (about 2.5 pH unit) as a result of ion exchange of surface H^+ ions for adsorbing nickel or copper ions. Note that the plateau-adsorbed values by pristine and oxidized samples do not differ substantially.

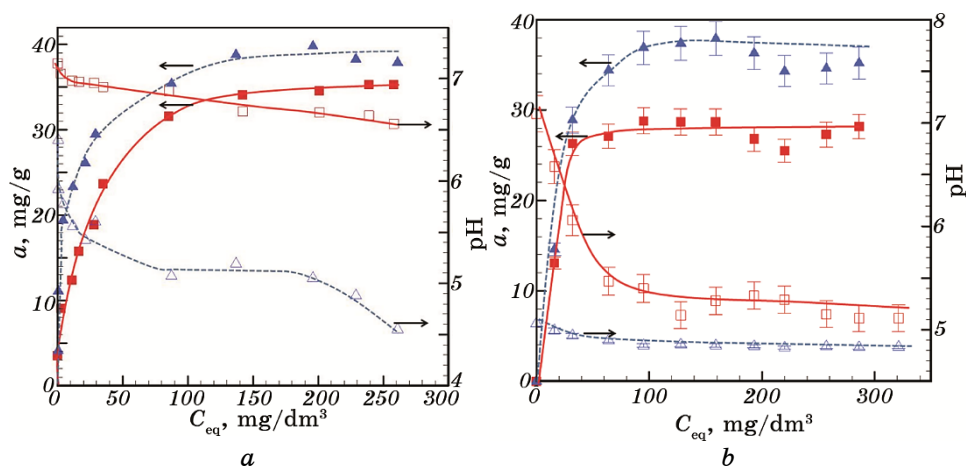


Fig. 6. Adsorption isotherms of the Ni(II) (a) and Cu(II) (b) ions by the as-prepared (squares) and oxidized (triangles) N-CNTs at ‘natural’ pH of the suspension (pH 5.0–6.0). In addition, the changes in the equilibrium pH of a 0.1% suspension because of ions’ adsorption are also shown.

Quite different changes in the equilibrium pH of N-CNT suspensions having various adjusted pH values and different adsorbed amounts of Ni(II) and Cu(II) ions were found. Addition of N-CNTs to the salt solutions in acidic media with adjusted pH (in the range of approximately pH 2–5 for as-prepared and pH 2–4 for oxidized samples) results in a measurable increase of the suspension equilibrium pH. For example, adsorption of Ni(II) in amount of 7.14 mg/g or 17.8 mg/g resulted in the rise of the adjusted/initial pH from 2.83 to 3.48 or 5.23 to 6.18 in the 0.1% N-CNT suspension, respectively (see Table 1). Similar rise of pH (up to 1.5–2.0 pH units) was observed in the oxidized N-CNT suspensions in acidic media in the event of either Ni(II) or Cu(II) adsorption. We attribute this rise in pH to the transfer of H⁺ ions from the solution to pyridine N-atoms on the N-CNTs surface, *i.e.*, we can hardly imagine the substitution of surface hydrogen ions by adsorbing copper ions in the presence of excess H⁺ ions (low pH) in the system. At higher pH values, this effect is overcompensated by the ion exchange of Cu(II) with surface H⁺ ions that gives a moderate drop in pH for pristine N-CNTs and a much bigger decrease of pH (up to 2.5 pH units) for the oxidized samples (Table). In alkali media, an additional release of H⁺ ions occurs because of hydrolysis and precipitation of Ni(II) or Cu(II) ions in the form of hydroxides.

Obviously, different mechanisms are governing the adsorption of Ni(II) and Cu(II) ions by N-CNTs. A release of H⁺ ions from the oxidized N-CNTs testifies the essential role of the ion exchange in binding the nickel or copper ions for this adsorbent; this mechanism

TABLE. Changes of the equilibrium pH ($\text{pH}_{\text{eq.}}$) of 0.1% N-CNT suspensions containing 29–31 mg of the Ni(II) or Cu(II) ions per 1 g carbon nanotubes at various initial/adjusted pH ($\text{pH}_{\text{adj.}}$) of the system (selected data).

Adsorption of Ni(II)						Adsorption of Cu(II)					
Pristine N-CNTs			Oxidized N-CNTs			Pristine N-CNTs			Oxidized N-CNTs		
$\text{pH}_{\text{adj.}}$	$\text{pH}_{\text{eq.}}$	a , mg/g	$\text{pH}_{\text{adj.}}$	$\text{pH}_{\text{eq.}}$	a , mg/g	$\text{pH}_{\text{adj.}}$	$\text{pH}_{\text{eq.}}$	a , mg/g	$\text{pH}_{\text{adj.}}$	$\text{pH}_{\text{eq.}}$	a , mg/g
2.83	3.48	7.14	2.84	3.18	9.5	2.02	2.08	6.13	2.03	2.09	12.1
4.20	5.43	14.5	4.11	4.93	18.0	2.93	3.18	9.71	2.43	2.99	22.4
5.23	6.18	17.8	5.36	5.23	18.1	4.20	5.64	25.4	4.84	3.72	32.5
6.58	6.50	17.7	6.38	5.26	18.4	5.76	5.73	33.3	5.95	3.96	31.5
8.32	7.04	18.3	8.25	5.60	20.2	6.71	5.86	34.7	6.58	5.00	54.6
8.77	7.64	20.2	8.77	6.58	27.7	8.96	6.62	59.9	8.86	6.45	60.9
11.3	9.70	28.8	11.2	7.74	28.2						

is supported by the FTIR data (Fig. 4). To estimate the contribution of this factor, we have compared the adsorbed amounts with changes of the solution pH, *i.e.*, the concentration of the substituted H^+ ions by copper or nickel ions from the surface. For example, adsorption of 31.5 mg/g or $4.9 \cdot 10^{-4}$ mole/g Cu(II) by oxidized N-CNTs resulted in a decrease of solution pH from 5.95 to 3.96, which corresponds to an appearance of roughly 10^{-4} M ions in the suspension of concentration 10 mg CNT/10 cm³ or 1.0 g CNT/dm³. This means that a part (approximately 20%) of Cu(II) ions is adsorbed *via* ion exchange with H^+ ions of the surface.

At the same time, the majority of copper ions are bound to the CNTs because of other type interactions, probably donor–acceptor interaction between the free electron pair of N-atoms of the surface and vacant *d*-orbital of the adsorbing ions. Similar calculations have shown that adsorption of 16.3 mg/g or $2.8 \cdot 10^{-4}$ mole/g Ni(II) by pristine N-CNTs, which decreased the solution pH from 8.32 to 7.04, resulted in appearance of $1.5 \cdot 10^{-7}$ mole H^+ ions in a suspension with 10 mg N-CNTs or $1.5 \cdot 10^{-5}$ mole H^+ ions per 1 g nanotubes. This comprises only 5% of the adsorbed amount of nickel ions. In the event of oxidized N-CNT adsorption of 18.4 mg/g of Ni(II), the drop in the system pH reached 1.12 pH unit, from 6.38 to 5.26 which corresponds to an increase in the H^+ concentration from $4 \cdot 10^{-6}$ mole/dm³ to $2 \cdot 10^{-5}$ mole/dm³, which is less than 10% of the adsorbed amount of Ni(II) ($3.2 \cdot 10^{-4}$ mole/g).

4. CONCLUSIONS

We describe and discuss in this paper the laws and mechanisms of adsorption of Ni(II) and Cu(II) ions by well characterized pristine and oxidized N-doped multi-walled carbon nanotubes (N-CNTs).

As demonstrated, the N-CNTs can serve for extraction of Ni(II) and Cu(II) ions from aqueous solution. The specific adsorption values (28–35 mg/g for copper and 35–40 mg/g for nickel) and degree of extraction (10–99% from solutions of equilibrium concentration of 580–5.0 mg/dm³) of these ions are comparable with those for the non-oxidized and oxidized multiwalled carbon nanotubes described in the literature. The main laws of adsorption observed can be summarized as follow: (i) adsorption reaches equilibrium value within 60 min; (ii) the degree of extraction of ions sharply increases with a decrease in their concentration, (iii) adsorption of Cu(II) and Ni(II) by as-prepared N-CNTs results in a moderate decrease in the pH value of the suspension (up to 1.5 pH unit) and in a considerable lowering the pH for oxidized samples (up to 2.5 pH unit); (iv) the adsorption isotherms can be described by the Langmuir equation; (v) at pH ≥ 6.5 for Cu(II) and pH ≥ 8.0 for Ni(II) a sharp in-

crease in adsorption took place. We consider that the laws described can be explained by accounting three types of binding of these ions to the N-CNTs surface: (i) ion-exchange between Cu(II) or Ni(II) ions and H^+ of surface functional groups, and this effect is more pronounced for the oxidized N-CNTs sample but does not make decisive contribution into adsorption; (ii) donor–acceptor interaction between the vacant d -orbital of adsorbing transition metal ions and N-atoms of the nanotubes matrix, and this effect seems to be universal and playing major role in the binding of transition metal ions to both as-prepared and oxidized samples surface; (iii) precipitation of $Cu(OH)_2$ or $Ni(OH)_2$ onto carbon nanotubes surface at hydroxides precipitation pH values.

REFERENCES

1. X. Ren, C. Chen, M. Nagatsu, and X. Wang, *Chem. Eng. J.*, **170**, Nos. 2–3: 395 (2011); <https://doi.org/10.1016/j.cej.2010.08.045>.
2. Y.-H. Li, S. Wang, J. Wei, X. Zhang, C. Xu, Z. Luan, D. Wu, and B. Wei, *Chem. Phys. Lett.*, **357**, Nos. 3–4: 263 (2002); [https://doi.org/10.1016/S0009-2614\(02\)00502-X](https://doi.org/10.1016/S0009-2614(02)00502-X).
3. K. Pyrzynska and M. Bystrzejewski, *Colloids Surf. A*, **362**: 102 (2010); <https://doi.org/10.1016/j.colsurfa.2010.03.047>.
4. M. V. Manilo, Z. Z. Choma, and S. Barany, *Colloid J.*, **79**, No. 2: 212 (2017); <https://doi.org/10.1134/S1061933X17020053>.
5. Y.-H. Li, S. Wang, Z. Luan, J. Ding, C. Xu, and D. Wu, *Carbon*, **41**: 1057 (2003); [https://doi.org/10.1016/S0008-6223\(02\)00440-2](https://doi.org/10.1016/S0008-6223(02)00440-2).
6. Ch. Chen and X. Wang, *Ind. Eng. Chem. Res.*, **45**, No. 26: 9144 (2006); <https://doi.org/10.1021/ie060791z>.
7. Sh. Yang, J. Li, D. Shao, J. Hu, and X. Wang, *J. Hazard. Mater.*, **166**, No. 1: 109 (2009); <https://doi.org/10.1016/j.jhazmat.2008.11.003>.
8. M. Kandah and J.-L. Meunier, *J. Hazard. Mater.*, **146**, Nos. 1–2: 283 (2007); <https://doi.org/10.1016/j.jhazmat.2006.12.019>.
9. Ch. Lu and Ch. Liu, *J. Chemical Technology and Biotechnology*, **81**, No. 12: 1932 (2006); <https://doi.org/10.1002/jctb.1626>.
10. F. Giannakopoulou, C. Haidouti, D. Gasparatos, I. Massasand, and G. Tsiakatouras, *Desalination and Water Treatment*, **57**, No. 25: 11623 (2016); <https://doi.org/10.1080/19443994.2015.1042069>.
11. A. Stafiej and K. Pyrzynska, *Separation and Purification Technology*, **58**: 49 (2007); <https://doi.org/10.1016/j.seppur.2007.07.008>.
12. L. Vanyorek, G. Muranszky, B. Fiser, E. Sikura, Zs. Hutkai, and B. Viskolcz, *J. Disp. Sci. Techn.*, **40**: 1 (2019); <https://doi.org/10.1080/01932691.2019.1637757>.
13. D. A. Bulushev, A. L. Chuvilin, V. I. Sobolev, S. G. Stolyarova, Y. V. Shubin, I. P. Asanov, A. V. Ishchenko, G. Magnani, M. Riccò, A. V. Okotrub, and L. G. Bulusheva, *J. Mat. Chem. A*, **5**: 10574 (2017); <https://doi.org/10.1039/C7TA02282D>.
14. G. P. Rao, Ch. Lu, and F. Su, *Separ. Purific. Techn.*, **58**: 224 (2007); <https://doi.org/10.1016/j.seppur.2006.12.006>.

15. M. A. Salam, Gh. Al-Zhrani, and S. A. Kosa, *Comptes Rendus Chimie*, **15**, No. 5: 398 (2012); <https://doi.org/10.1016/j.crci.2012.01.013>.
16. A. Gadhawe and J. Waghmare, *International J. Chemical Sci. Applications*, **5**, No. 2: 56 (2014).
17. Zh. Gao, T. J. Bandosz, Z. Zhao, M. Hanand, and J. Qiu, *J. Hazardous Materials*, **167**, Nos. 1–3: 357 (2009); <https://doi.org/10.1016/j.jhazmat.2009.01.050>.
18. L. Vanyorek, R. Mészáros, and S. Bárány, *Colloids and Surfaces A*, **448**: 140 (2014); <https://doi.org/10.1016/j.colsurfa.2014.01.078>.
19. S. Barany, N. Kartel', and R. Meszaros, *Colloid J.*, **76**: 509 (2014); <https://doi.org/10.1134/S1061933X14050020>.
20. S. Gomez, N. M. Rendtorff, E. F. Aglietta, Y. Sakka, and G. Suarez, *Applied Surface Sci.*, **379**: 264 (2016); <https://doi.org/10.1016/j.apsusc.2016.04.065>.
21. K. Csobán, M. Párkányi-Berka, P. Joó, and Ph. Behrab, *Colloids and Surfaces A: Physicochemical and Engineering Aspects*, **141**, No. 3: 347 (1998); [https://doi.org/10.1016/S0927-7757\(98\)00244-1](https://doi.org/10.1016/S0927-7757(98)00244-1).
22. K. Csobán and P. Joó, *Colloids and Surfaces A: Physicochemical and Engineering Aspects*, **151**, Nos. 1–2: 97 (1999); [https://doi.org/10.1016/S0927-7757\(98\)00421-X](https://doi.org/10.1016/S0927-7757(98)00421-X).
23. J. Lakatos, S. D. Brown, and C. E. Snape, *Fuel*, **81**, No. 5: 691 (2002); [https://doi.org/10.1016/S0016-2361\(01\)00159-4](https://doi.org/10.1016/S0016-2361(01)00159-4).
24. M. Ajmal, R. A. K. Rao, R. Ahmad, J. Ahmad, and L. A. K. Rao, *J. Hazardous Materials*, **87**, Nos. 1–3: 127 (2001); [https://doi.org/10.1016/S0304-3894\(01\)00234-5](https://doi.org/10.1016/S0304-3894(01)00234-5).
25. M. V. Manilo, Z. Z. Choma, and S. Barany, *Colloid J.*, **79**, No. 2: 212 (2017); <https://doi.org/10.1134/S1061933X17020053>.
26. K. A. Burkov, L. S. Lilič, and L. G. Sillien, *Acta Chem. Scandinavia*, **19**: 14 (1965); <https://doi.org/10.3891/acta.chem.scand.19-0014>.
27. D. Novak-Adamic, B. Cosovic, H. Bilinski, and M. Branica, *J. Inorg. Nucl. Chem.*, **35**, No. 7: 2371 (1973); [https://doi.org/10.1016/0022-1902\(73\)80303-3](https://doi.org/10.1016/0022-1902(73)80303-3).